KNEE

Medial meniscus posterior root tear causes swelling of the medial meniscus and expansion of the extruded meniscus: a comparative analysis between 2D and 3D MRI

Yoshiki Okazaki[1] · Takayuki Furumatsu[1] · Takuya Yamaguchi[2] · Yuya Kodama[3] · Yusuke Kamatsuki[1] · Shin Masuda[1] · Yuki Okazaki[1] · Takaaki Hiranaka[1] · Ximing Zhang[1] · Toshifumi Ozaki[1]

Abstract

Purpose This study aimed to clarify the advantages of three-dimensional (3D) magnetic resonance imaging (MRI) over two-dimensional (2D) MRI in measuring the size of the medial meniscus (MM) and to analyse the volumes of MM and the extruded meniscus in patients with MM posterior root tear (MMPRT), at 10° and 90° knee flexion.

Methods This study included 17 patients with MMPRTs and 15 volunteers with uninjured knees. The MMs were manually segmented for 3D reconstruction; thereafter, the extruded part separated from the tibial edge was determined. The length, width, height, and extrusion of MM were measured by the 2D and 3D methods, and compared. The MM volume, extruded meniscus volume, and their ratio were also calculated using 3D analysis software in the two groups.

Results The estimated length and posterior height of MM were larger with 3D MRI than with 2D MRI measurements. The MM volume was significantly greater in MMPRT knees than in normal knees, with increasing MM height. In MMPRT knees, the mean volume of the extruded meniscus and its ratio significantly increased by 304 mm^3 ($p = 0.02$) and 9.1% ($p < 0.01$), respectively, during knee flexion.

Conclusions This study demonstrated that 3D MRI could estimate the precise MM size and that MMPRT caused swelling of the meniscus due to the increased thickness in the posteromedial part. The clinical significance of this study lies in its 3D evaluation of MM volume, which should help the surgeon understand the biomechanical failure of MM function and improve MMPRT repair technique.

Level of evidence III.

Keywords Medial meniscus · Posterior root tear · Osteoarthritis · Meniscal volume · Medial extrusion · Three-dimensional magnetic resonance imaging · Flexed-knee position

Abbreviations

2D	Two-dimensional
3D	Three-dimensional
CI	Confidence interval
ICC	Intra-class correlation coefficient
Iso FSE	Isotropic resolution fast spin-echo
LM	Lateral meniscus
MM	Medial meniscus
MMBW	Medial meniscus body width
MMEV	Medial meniscus extrusion volume
MML	Medial meniscus length
MMME	Medial meniscus medial extrusion
MMPE	Medial meniscus posterior extrusion
MMPH	Medial meniscus posterior height
MMPRT	Medial meniscus posterior root tear
MMRV	Medial meniscus remaining volume
MMV	Medial meniscus volume
MPL	Medial plateau width
MRI	Magnetic resonance imaging
OA	Osteoarthritis
TPW	Total plateau width

Introduction

Medial meniscus (MM) posterior root tear (MMPRT) is defined either as a complete radial tear that is located within 9 mm of the MM posterior insertion or as a bony avulsion of the root attachment [1, 21]. MMPRT results in notable MM extrusion (MME) and gap formation at the root avulsion site when compressive loads are applied at the knee, representing functional failure of the load transmission into hoop strain [18, 26, 30]. Many studies reported that an MME of ≥ 3 mm on magnetic resonance imaging (MRI) was significantly associated with articular cartilage degeneration [20, 33].

One of the main disadvantages of two-dimensional (2D) MRI measurements is that they rely on particular coronal and sagittal slices, which makes it difficult to precisely define the meniscus size, including its length, width, and height in its curved regions (i.e., body and anterior and posterior horns) [23, 31, 35]. Thus, a three-dimensional (3D) MRI-based technology has been developed to measure the meniscus size and its position relative to the tibia [2–4]. Recently, 3D MRI has been used to determine the meniscal volume and quantify the entire meniscus [9]. However, it is largely unclear whether the 3D method is superior to the 2D method.

Studies involving the measurement of meniscal volume have been conducted for knees with osteoarthritis (OA). Wirth et al. reported that the MM volume (MMV) was greater in OA than in non-OA knees [35], while cohort studies showed that MMVs did not differ between OA and non-OA knees [2, 34], indicating the existence of variations in MMV. A recent analysis confirmed that the volume of the extruded meniscus from the tibia was greater in OA knees than in non-OA knees [9]. However, to our knowledge, no study has compared the volumes of the entire MM and extruded MM between MMPRT and normal knees in the knee-flexed position.

The purpose of this study was to clarify the benefit of 3D MRI by examining differences in MM size between 2D and 3D measurements and to analyse the volumes of entire MM and extruded MM in MMPRT and normal knees, at 10° and 90° of knee flexion. Our hypotheses were as follows: (1) 3D MRI would provide the precise length, width, and height of the meniscus; (2) entire MMV would not differ between MMPRT knees and normal knees; and (3) MM extrusion volume (MMEV) would be larger in MMPRT knees than in normal knees. This study involved a novel 3D method for evaluating MMVs, which could provide clinical information that reveals altered joint biomechanics in MMPRT knees.

Materials and methods

From August 2017 to September 2018, 32 knees in 32 subjects who underwent MRI examinations at Okayama University Hospital were included. This retrospective study consisted of 17 female patients with MMPRT and 15 female volunteers with normal (uninjured) knees. The MMPRT patients were found to passively have characteristic MRI findings (ghost/cleft/radial tear signs of MM posterior root from the attachment and the giraffe neck sign [7, 12]) at the initial MRI and were limited to those who provided informed consent for additional 3D MRI examination. Of these, patients who had radiographic knee OA with Kellgren-Lawrence grade III or higher and a previous history of meniscus injuries were excluded. Female nurses in our hospital were recruited in this study as volunteers and were limited to middle-aged and elderly women to match the characteristics of the MMPRT patients. To compare the knee size in both groups, the total plateau width (TPW) and medial plateau length (MPL) were measured on MRI-based coronal and sagittal planes [23, 31]. TPW was defined as the distance from the most medial to the lateral aspect of the tibia. MPL was measured as the distance of the maximal anteroposterior length of the medial plateau. The mean duration from MMPRT onset to MRI examination was 78 (range, 13–235) days. MMPRT types were identified by careful arthroscopic examinations according to the LaPrade classification as follows: type 1 and 2 tears were partial and complete radial tears, respectively, within 9 mm of the centre of the root attachment; type 3 tears were bucket-handle tears; type 4 tears were complex oblique meniscal tears extending into the root attachment; and type 5 tears were avulsion fractures of the meniscal root attachment [22].

### MRI protocol and 3D model preparation

MRI was performed using the Oasis 1.2 Tesla (Hitachi Medical, Chiba, Japan), with a coil in the 10° and 90° knee-flexed positions in a non-weight-bearing condition (Figs. 1a, b, 2a, b). Knee flexion angle was measured using a knee goniometer, with the knee held in neutral rotation. Multiplanar images were acquired using proton density-weighted isotropic resolution fast spin-echo (iso FSE, Hitachi Medical) sequence with continuous 1-mm slice thickness. The 3D FSE images were applied in the sagittal and coronal planes with repetition time/echo time, 600/96 ms; matrix, 224×224; field of view, 18 cm; 1 average; echo-train length, 24; bandwidth, ± 98.1 kHz; and scanning time, 4.8 min.

Data on the femur and tibia were extracted semi-automatically with the voxel density threshold for the surface
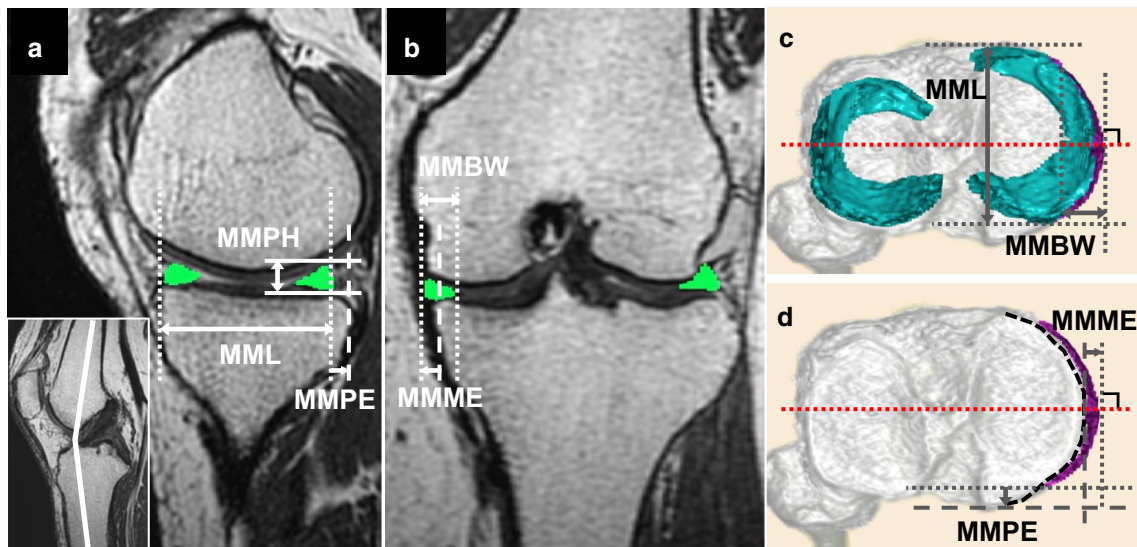
Fig. 1 2D and 3D segmentations using proton density-weighted iso FSE image, at 10°. **a** The 2D sagittal plane with the longest MML (double-headed arrow), MMPH (vertical double-headed arrow), and MMPE (arrow). The anterior and posterior margins of MM (dotted lines), the highest and lowest borders of MM (solid lines), and posterior edge of the tibia plateau (dashed line). **b** The 2D coronal plane with the greatest MMBW (double-headed arrow) and MMME (arrow). The inner and outer margins of MM (dotted lines), the outer edge of the tibia (dashed line). **c** The 3D model of the whole meniscus covering the tibial plateau (cyan area) and extrusion area (purple area). A reference line (red dotted line) was drawn passing through the tibial intercondylar spines. MML (perpendicular double-headed grey arrow) and MMBW (double-headed grey arrow). **d** The extrusion area (purple area) was defined as the region separated by the black dashed line, which represents the circumference points of the medial tibia. MMME (grey arrow) was the distance from the most medial edge of the tibia (dashed grey line) to MM (dotted grey line). MMPE (grey arrow) was the distance from the most posterior edge of the tibia (dashed grey line) and MM (dotted grey line)
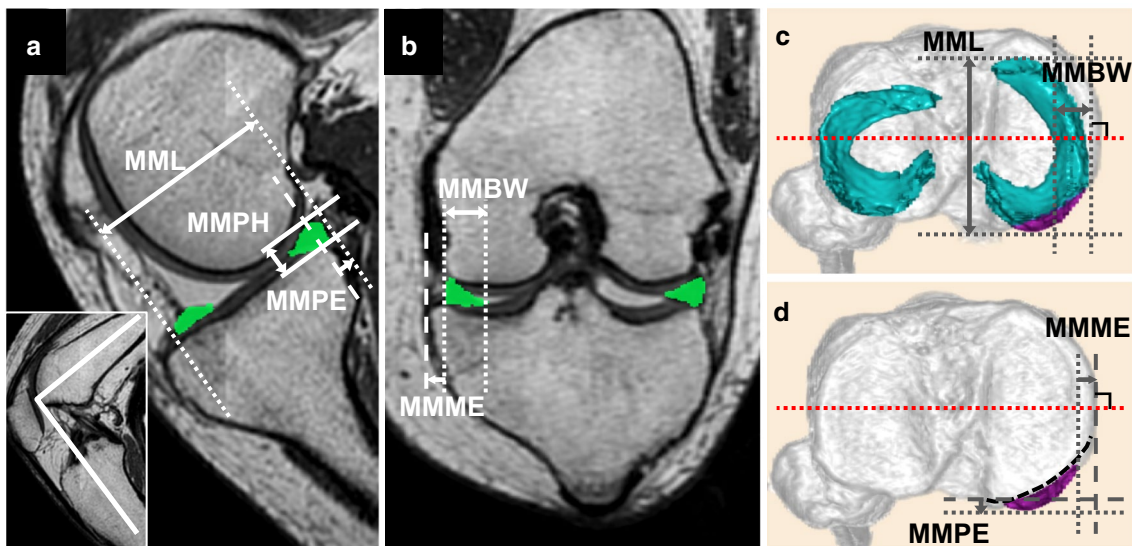
Fig. 2 2D and 3D segmentations using proton density-weighted iso FSE image, at 90°. **a** The 2D sagittal plane with the longest MML (double-headed arrow), MMPH (vertical double-headed arrow), and MMPE (arrow). **b** The 2D coronal plane with the greatest MMBW (double-headed arrow) and MMME (arrow). **c** The 3D model of the whole meniscus (cyan and purple areas) and tibial plateau. A refer-ence line (red dotted line) along the tibial intercondylar spines. MML (perpendicular double-headed grey arrow) and MMBW (double-headed grey arrow). **d** The extruded area from the tibial posterior edge (purple area). MMME (grey arrow) and MMPE (perpendicular grey arrow)

definition using the 3D image analysis workstation SYN-APSE VINCENT® (Fuji Medical System, Tokyo, Japan). Segmentations of the meniscus using the texture tracing technique [17, 29] were performed manually by a radiologic technologist (TY) and two orthopaedic surgeons (YoO and TF). After the segmentation process, three kinds of 3D reconstructed meniscus were obtained by the volume-rendering method [8, 25] (Figs. 1c, d, 2c, d).

Comparative analysis between the 2D and 3D measurements

The conventional 2D measurement was performed using a simple MRI-based meniscal sizing method [13, 24]. A posterior condylar line was drawn passing on the most posterior edge of the femoral condyles. The sagittal and coronal planes were created vertical and parallel to the posterior condylar line, respectively. The 2D parameters were measured in the sagittal plane where the MM length (MML) was longest (Figs. 1a, 2a), and in the coronal plane where the MM body width (MMBW) was widest (Figs. 1b, 2b) MML was defined as the length from the anterior to the posterior edge of MM. MMBW was measured from the outer to the inner border of MM. MM posterior height (MMPH) was defined as the height from the lowest to the highest point in the posterior segment of MM. MM medial extrusion (MMME) was measured from the medial edge of the tibia to the outer border of MM in the coronal plane. MM posterior extrusion (MMPE) was defined as the distance from the posterior edge of the tibia to the posterior border of MM in the sagittal plane.

The 3D-based measurement was conducted by applying a method similar to the sizing technique for meniscal allografts [23, 31]. A 3D model of the meniscus was observed from above the axial plane, which was taken parallel to the tibial plateau (Figs. 1c, 2c). First, a reference line was created intersecting the tibial intercondylar spines. The anterior and posterior borders of MM were determined parallel to the reference line. MML was the distance measured from the anterior to the posterior border of MM. MMBW was defined as the width from the outermost border to the innermost border of MM. The MME area was created by identifying the outline of the tibia plateau, and cutting the inner part of MM through the outline, as previously described [9] (Figs. 1d, 2d). MMME was measured as the distance from the medial edge of the tibia to the MM outer edge. MMPE was defined as the distance from the posterior edge of the tibia to the posterior border of MM. In addition, MMPH was defined as the height from the lowest to the highest point in the MM posterior segment on the coronal plane perpendicular to the tibial plateau. The average of the 3D measurements recorded by the three observers was calculated and compared with the average of the 2D measurements.

To evaluate the repeatability of the above parameters, test–retest reliability calculations were conducted at time intervals of > 10 weeks, using the intra-class correlation coefficient (ICC), with the 95% confidence interval (CI).

Volume analysis of MM and the extruded meniscus

Volume measurement of the meniscus was performed via voxel counting, which was calculated by the summation of all voxel volumes lying within the boundaries; this has been reported as a valid and accurate method of volume analysis [35]. All 3D images in the present study had a reconstructed matrix size of 512×512, pixel size of 0.352 mm^2, and slice thickness of 1 mm. The volume of each voxel was 0.124 mm^3, according to the following formula: $1 \times 0.352 \times 0.352$. After visual confirmation of the exact segmentation of MM, the SYNAPSE VINCENT® software accomplished the MMV measurements automatically.

MMEV was defined as the volume of the extruded meniscus beyond the inner articular part of MM (Figs. 1d, 2d). The MMEV ratio was calculated as MMEV divided by MMV to adjust for individual differences. In addition, the negative MMV in the inner articular part was determined as the MM remaining volume (MMRV). The MMRV ratio (MMRV/MMV × 100) was also calculated.

The 3D parameters (MML, MMBW, MMPH, MMME, and MMPE) and these volume measurements were compared between MMPRT knees and normal knees at 10° and 90° of knee flexion.

Reliability evaluation of the 3D segmentation

A radiologic technologist and two orthopaedic surgeons (YoO and TF) retrospectively segmented MM and defined the MME area manually. The technologist segmented MM and the MME area in a blinded manner, at 12 weeks after the first examinations, followed by automatic volume calculations. The inter- and intra-observer reliabilities of the MRI volume measurements were assessed using the ICC. An ICC of ≥ 0.75 was considered excellent, ≥ 0.60 to < 0.75 good; ≥ 0.40 to < 0.60 fair, and < 0.40 poor [32].

Validation study of meniscal volume

Six intact lateral menisci (LMs) were obtained during total knee arthroplasty in patients (2 women and 4 men) with medial compartmental OA of the knee. The MRI scan of each LM was taken using the abovementioned 3D protocol. Manual segmentation via the SYNAPSE VINCENT® software was performed by the three observers and the calculation values averaged. Thereafter, the 3D MRI-based volume was compared to its water suspension volume [14]. The suspension method has been shown to be an accurate

technique for volume measurement, using Archimedes' principle, which involves suspending an object (meniscus) in a water-filled container placed on electronic weight scales. Each water suspension volume measurement was repeated three times, and the values were averaged.

This study was approved by the Institutional Review Board of Okayama University (ID number of the approval: 1857) and written informed consent was obtained from all subjects before the MRI examinations.

Statistical analysis

IBM SPSS Statistics version 25.0 (IBM Corp., Armonk, NY, USA) was used for all statistical analyses. The differences in 2D vs. 3D MRI measurements were examined using paired *t*-tests. The Mann–Whitney *U*-test was used to compare the 3D MRI measurements between the two groups and the changes from 10° to 90° knee flexion. Data are presented as mean ± standard deviation and significance was set at $p < 0.05$. The correlation of difference in the validation study was analysed using parametric (Pearson r) correlation coefficients. The sample size was estimated using a power of 80% and α of 0.05. The samples of MML and MMPH needed in the first comparative study was 15 in each group. The required sample size for MMPH and MMV in the second comparative study was 15 in each group.

Results

Characteristics of study participants

The two groups did not differ significantly (ns) with regard to age, height, body weight, and body mass index (Table 1). There were also no significant differences in terms of knee sizes involving TPW and MPL. The MMPRT groups included 15 radial tears (type 2) and two oblique tears (type 4).

Comparative analysis between the 2D and 3D measurements

MMPRT knee

At 10° of knee flexion, MML was significantly smaller in the 2D measurement than in the 3D measurement (mean difference; 1.7 ± 1.0 mm, $p < 0.001$) (Table 2). At 90° of knee flexion, MML and MMPH were significantly smaller in the 2D measurement than in the 3D measurement (mean difference; 1.6 ± 1.3 mm, $p < 0.001$ and 1.4 ± 1.0 mm, $p = 0.001$, respectively), while MMME and MMPE were greater in the 2D measurement than in the 3D measurement.

Normal knee

MML was significantly smaller in the 2D measurement than in the 3D measurement at 10° and 90° of knee flexion (mean difference; 1.2 ± 0.8 mm, $p = 0.011$ and 1.8 ± 1.3 mm, $p = 0.001$, respectively) (Table 2).

Measurement repeatability

The overall test–retest reliability data are shown in Table 3. Excellent repeatability was demonstrated in all 3D MRI measurements. Most ICCs were higher in 3D MRI measurements than in 2D MRI measurements.

Differences in the 3D measurements between MMPRT and normal knees

Flexion angle of 10°

MMME, MMV, MMEV, and MMEV ratios were significantly greater in MMPRT knees than in normal knees, while the MMRV ratio was significantly lower in MMPRT knees (Table 4).

Table 1 Patient demographics including mean values and number of patients

Variables	MMPRT ($n = 17$)	Normal ($n = 15$)	*P* value
Age, years	62.1 ± 9.6	57.1 ± 5.5	ns
Height, m	1.54 ± 0.05	1.56 ± 0.04	ns
Body weight, kg	59.3 ± 8.3	56.5 ± 8.4	ns
Body mass index, kg/m^2	25.0 ± 2.7	23.3 ± 3.3	ns
Total plateau width, mm	68.3 ± 2.5	68.5 ± 2.4	ns
Medial plateau length, mm	45.1 ± 2.6	45.8 ± 1.8	ns
LaPrade classification (type 1/2/3/4/5)	0/15/0/2/0	–	–

MMPRT medial meniscus posterior root tear, *ns* non-significant

Significance was determined with use of the Mann-Whitney *U* test. $p < 0.05$

Table 2 Comparative analysis between 2D and 3D measurements at a knee flexion angle of 10° and 90°

	MMPRT				Normal			
	2D MRI measurement	3D MRI measurement	Difference	P value	2D MRI measurement	3D MRI measurement	Difference	P value
Flexion 10° (mm)								
MML	43.1 ± 2.4	44.8 ± 2.4	1.7 ± 1.0	< 0.001*	41.6 ± 1.7	42.8 ± 1.8	1.2 ± 0.8	0.011*
MMBW	9.4 ± 1.2	9.8 ± 1.3	0.4 ± 0.5	ns	8.7 ± 1.0	9.0 ± 0.9	0.4 ± 0.6	ns
MMPH	7.1 ± 0.7	7.3 ± 0.7	0.2 ± 0.2	ns	6.3 ± 0.7	6.3 ± 0.7	0 ± 0.1	ns
MMME	3.5 ± 0.7	3.4 ± 0.7	− 0.1 ± 0.2	ns	1.4 ± 0.6	1.4 ± 0.6	0 ± 0.8	ns
MMPE	− 2.9 ± 2.1	− 2.9 ± 2.0	0 ± 0.4	ns	− 3.6 ± 0.6	− 3.7 ± 0.5	− 0.2 ± 0.4	ns
Flexion 90° (mm)								
MML	44.3 ± 3.1	45.9 ± 2.8	1.6 ± 1.3	< 0.001*	40.3 ± 2.0	42.0 ± 1.7	1.8 ± 1.3	0.001*
MMBW	10.2 ± 1.5	11.0 ± 1.5	0.8 ± 0.6	ns	9.0 ± 1.2	9.3 ± 1.3	0.3 ± 0.6	ns
MMPH	7.7 ± 1.4	9.1 ± 1.4	1.4 ± 1.0	0.001*	6.8 ± 0.7	7.1 ± 0.8	0.3 ± 0.4	ns
MMME	2.8 ± 1.6	2.4 ± 1.2	− 0.5 ± 0.6	ns	0.1 ± 0.8	0.2 ± 0.8	0.1 ± 0.7	ns
MMPE	3.6 ± 1.2	3.4 ± 1.3	− 0.2 ± 0.3	ns	1.3 ± 0.8	1.3 ± 0.8	0.1 ± 0.4	ns

2D two-dimensional, *3D* three-dimensional, *MRI* magnetic resonance imaging, *MMPRT* medial meniscus posterior root tear, *MML* medial meniscus length, *MMBW* medial meniscus body width, *MMPH* medial meniscus posterior height, *MMME* medial meniscus medial extrusion, *MMPE* medial meniscus posterior extrusion, *ns* non-significant

*Significance was determined with use of paired *t* test. $p < 0.05$

Table 3 Test–retest reliabilities of MRI measurements

	2D MRI measurement	3D MRI measurement
Flexion 10° (mm)		
MML	0.91 (0.77–0.96)	0.98 (0.96–0.99)
MMBW	0.80 (0.54–0.92)	0.99 (0.97–1.00)
MMPH	0.81 (0.55–0.93)	0.90 (0.93–0.96)
MMME	0.91 (0.78–0.97)	0.92 (0.80–0.97)
MMPE	0.95 (0.88–0.98)	0.99 (0.98–1.00)
Flexion 90° (mm)		
MML	0.94 (0.83–0.98)	0.97 (0.91–0.99)
MMBW	0.85 (0.65–0.94)	0.96 (0.89–0.99)
MMPH	0.92 (0.79–0.97)	0.96 (0.89–0.98)
MMME	0.94 (0.85–0.98)	0.95 (0.88–0.98)
MMPE	0.98 (0.95–0.99)	0.95 (0.87–0.98)

The values are given as the intra-class correlation coefficient, with the 95% confidence interval

2D two-dimensional, *3D* three-dimensional, *MRI* magnetic resonance imaging, *MMPRT* medial meniscus posterior root tear, *MML* medial meniscus length, *MMBW* medial meniscus body width, *MMPH* medial meniscus posterior height, *MMME* medial meniscus medial extrusion, *MMPE* medial meniscus posterior extrusion

Flexion angle of 90°

MMPH, MMME, MMPE, MMV, MMEV, and MMEV ratios were significantly greater in MMPRT knees than in normal knees (Table 4). In contrast, MMRV and MMRV ratios were smaller in MMPRT knees than in normal knees.

Volume changes from 10° to 90° knee flexion

There was no significant difference in MMV between 10° and 90° knee flexion. MMEV and MMEV ratios in the MMPRT knee were significantly increased ($p = 0.020$ and 0.001, respectively) (Fig. 3), while MMRV ratio in the MMPRT knee was significantly decreased by 9.1% ($p = 0.001$).

Figure 4 shows representative cases in both groups. At 10° knee flexion, MME areas were observed between the anterior and medial parts of the MM (Fig. 4a, b). However, at 90° knee flexion, compared to the normal knee, the MM posterior root in the MMPRT knee was widely detached and the MME area was translocated to the posteromedial direction of MM (Fig. 4c, d). In addition, the extruded MM in MMPRT knees was thickened.

Reliability evaluation of the 3D segmentation

Inter-observer reliability

The ICC of MMV at 10° and 90° knee flexion was 0.89 (95% CI 0.75–0.96) and 0.85 (95% CI 0.65–0.94), respectively. The ICC of MMEV at 10° and 90° knee flexion was 0.86 (95% CI 0.67–0.95) and 0.84 (95% CI 0.63–0.94), respectively.

Table 4 3D MRI measurements in MMPRT and normal knees at a knee flexion angle of 10° and 90°

	Flexion 10°			Flexion 90°		
	MMPRT	Normal	*p* value	MMPRT	Normal	*p* value
MML (mm)	44.8 ± 2.4	42.8 ± 1.8	ns	45.9 ± 2.8	42.0 ± 1.7	ns
MMBW (mm)	9.8 ± 1.3	9.0 ± 0.9	ns	11.0 ± 1.5	9.3 ± 1.3	ns
MMPH (mm)	7.3 ± 0.7	6.3 ± 0.7	ns	9.1 ± 1.4	7.1 ± 0.8	< 0.001*
MMME (mm)	3.4 ± 0.7	1.4 ± 0.6	< 0.001*	2.4 ± 1.2	0.2 ± 0.8	< 0.001*
MMPE (mm)	− 2.9 ± 2.0	− 3.7 ± 0.5	ns	3.4 ± 1.3	1.3 ± 0.8	< 0.001*
MMV (mm³)	2953 ± 637	2406 ± 541	0.018*	3014 ± 413	2468 ± 433	0.002*
MMEV (mm³)	763 ± 304	260 ± 209	< 0.001*	1067 ± 337	205 ± 159	< 0.001*
MMEV ratio (%)	26.0 ± 9.9	9.8 ± 6.5	< 0.001*	35.1 ± 8.8	7.8 ± 5.4	< 0.001*
MMRV (mm³)	2190 ± 564	2146 ± 388	ns	1948 ± 305	2262 ± 345	ns
MMRV ratio (%)	74.0 ± 9.9	90.2 ± 6.5	< 0.001*	64.9 ± 8.8	92.2 ± 5.4	< 0.001*

3D three-dimensional, *MRI* magnetic resonance imaging, *MMPRT* medial meniscus posterior root tear, *MML* medial meniscus length, *MMBW* medial meniscus body width, *MMPH* medial meniscus posterior height, *MMME* medial meniscus medial extrusion, *MMPE* medial meniscus posterior extrusion, *MMV* medial meniscus volume, *MMEV* medial meniscus extrusion volume, *MMRV* medial meniscus remaining volume

*Significance was determined with use of the Mann-Whitney *U* test. *p* < 0.05

Fig. 3 The changes in 3D MRI-based volume measurements in each group, from 10° to 90° knee flexion. **a** MMV, **b** MMEV, **c** MMEV ratio (100 × MMEV/MMV). *p < 0.05
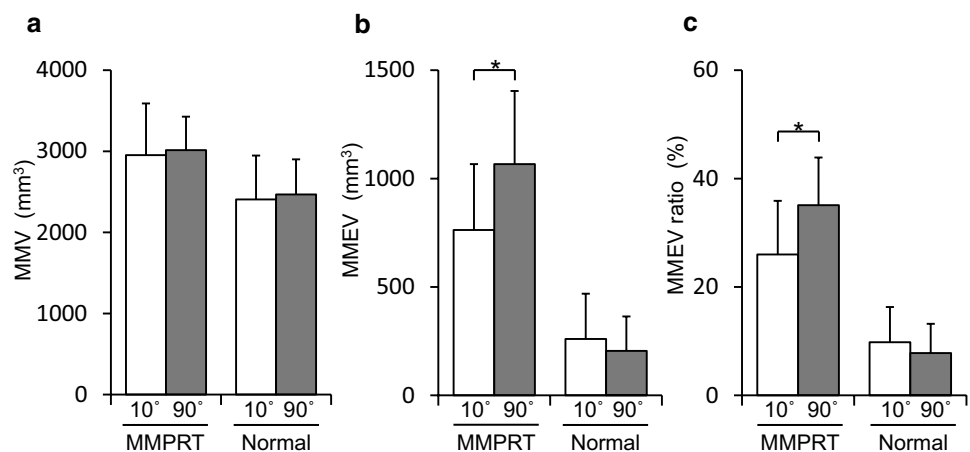
Intra-observer reliability

The ICC of MMV at 10° and 90° knee flexion was 0.96 (95% CI 0.90–0.99) and 0.89 (95% CI 0.69–0.96), respectively. The ICC of MMEV at 10° and 90° knee flexion was 0.90 (95% CI 0.72–0.97) and 0.89 (95% CI 0.68–0.96), respectively.

Validation analysis of the meniscus volume

The mean volume of the removed LM was 3016 ± 758 mm³ in the water suspension measurements and 2901 ± 606 mm³ in the 3D MRI measurements. An excellent correlation of coefficients was observed (*r* = 0.98). The mean absolute error between the two volume measurements was 4.6%.

Discussion

This comparative analysis demonstrated that 2D MRI measurement underestimated MM size and that 3D MRI achieved a higher measurement accuracy than 2D MRI. A major benefit of 3D MRI could be its ability to estimate the precise size and shape of the entire meniscus as indicated by the excellent repeatability shown in this study. In addition, to our knowledge, this is the first study to apply the SYNAPSE VINCENT® to the analysis of the meniscal volume. The present validation study showed an excellent correlation between the volume measurement in our study and that derived from Archimedes' principle. Moreover, the absolute error was low and was superior to that in the study of Bowers et al. (MM; 4.6%, LM; 7.9%) [5]. These

MMPRT   Normal

Flexion 10°

a   b

MMPH   MMPH

Flexion 90°

c   d

MMPH   MMPH

Fig. 4 Two cases involving a 60-year-old female patient with MMPRT (**a**, **c**) and a 59-year-old healthy woman with a normal knee (**b**, **d**). The purple area represents the MME area and the cyan area shows the inner part of the whole meniscus. The inlets below show the posterior part of the meniscus and MMPH measurements (double-headed arrows), on the coronal reconstructed image. **a** The MME area in the MMPRT case located along the medial part of the medial tibial plateau at 10° knee flexion. **b** The extrusion of normal MM was not widely recognised. **c** The MM posterior root in the MMPRT case was separated from the posterior attachment. The MME area spread to the posteromedial direction with increasing MMPH. **d** The normal MM was stabilised and MME partially lay on the posteromedial area
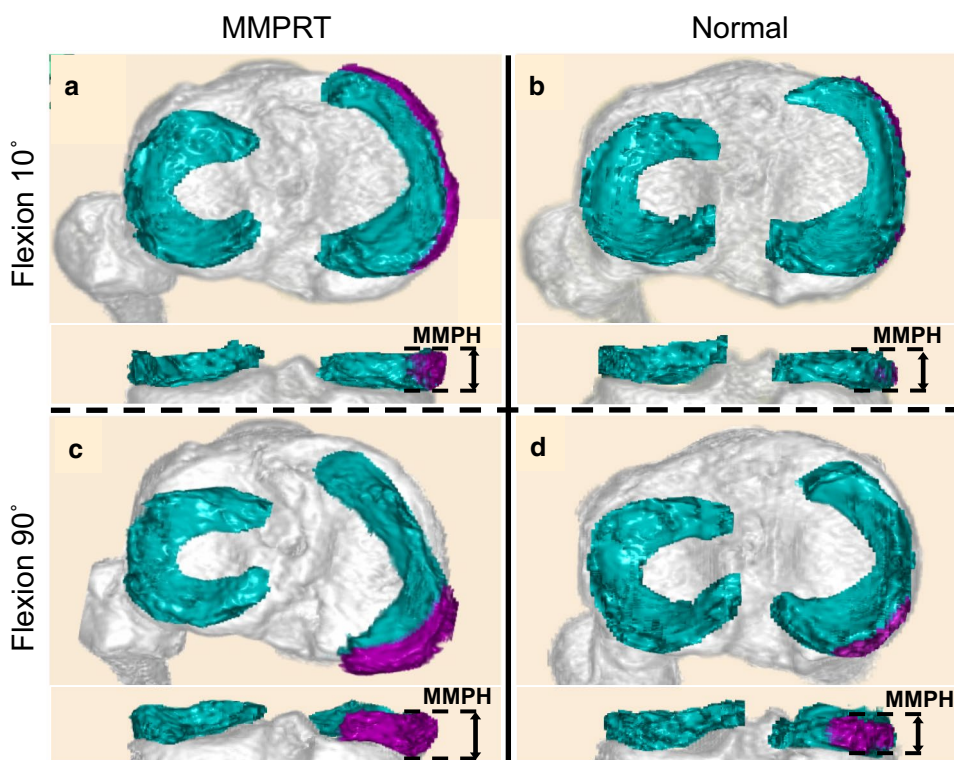
results indicate that the Vincent method is accurate for estimating the meniscal volume.

Previous studies that directly compared 2D MRI with cadaveric meniscus sizing demonstrated various differences in measurements. Shaffer et al. showed that only 37% of the 2D MRI measurements were accurate to within 2 mm of the true meniscal dimensions [31]. Carpenter et al. also found that conventional MRI consistently underestimated MML (mean error 2.6 mm) [6]. Conversely, in this study, the 3D measurement with larger MML is suggestive of approaching the precise length of the MM. Interestingly, we also discovered that 2D MRI underestimated MMPH in the MMPRT knee, especially at 90° knee flexion. In fact, the meniscal deformation was visualised in the 3D reconstructed model (Fig. 4), which demonstrated that the extruded MM expanded to the posteromedial direction with increasing meniscus thickness. This implies that 2D MRI, which relied on coronal and sagittal images, could not accurately evaluate the meniscus height and extrusion in the posteromedial region.

One important finding is that MMV was larger in the MMPRT knee than in the normal knee, thus contradicting the second hypothesis in the present study. The large MMV could have been due to the greater values of MML, MMBW, and MMPH in MMPRT (Table 4). A previous 3D study of OA knees demonstrated that meniscal thickness and width were significantly greater in OA knees than in non-OA knees [35]. The reason for this is that

medial compartmental OA increases the load on the MM, which is then displaced externally due to the loss of hoop tension and high biomechanical stress. Hence, MM is squeezed towards the unloaded outer joint, which may cause swelling [34]. It is conceivable that the same phenomenon occurred in the MMPRT knee with a disrupted hoop-strain mechanism. On the other hand, a histological analysis reported that a degenerative change in the posterior horn might precede complete MMPRT [28]. This analysis also showed that the collagen architecture was disorganised with the extent of the tear and that the widening of the root was observed in partial and complete tears. Therefore, a potential explanation is that MM swelling may exist before the occurrence of MMPRT.

An MRI analysis showed that during knee extension to deep flexion, the posterior translation of normal MM (3.3 ± 1.5 mm) was less than that of LM due to the strong attachment on the MM posterior root [36]. Recent open MRI studies have also shown that the MM posterior horn had a buttress effect and a more convex shape by compression force on the posterior condyle at 90° knee flexion [15, 24]. In contrast, the present study showed that MMPE in the MMPRT knee increased by 6.3 mm (or 6.5 mm) from 10° to 90° knee flexion, and that MMEV and MMEV ratio were greater than in the normal knee. Thus, we believe that the posterior femoral condyle compresses the torn MM in the posteromedial direction and the unloaded MM margin becomes thicker. Of note, this study showed the reduction

of MMRV in the MMPRT knee, suggesting the loss of MM function as a load transmitter [26, 27, 30].

There were several limitations to the present study. First, only a few subjects could be evaluated because of the discomfort involved in keeping the knee flexed for about 50 min during MRI. Second, the 3D MRI measurement could not be compared with the true meniscus size, such as obtained using cadaveric knees. Further studies are needed to verify the accuracy of 3D meniscal sizing. Third, the MMV measurements were conducted without joint loading; hence, the magnitude of MMEV might have been underestimated. To assess the mechanical change in MMV under load conditions will be necessary. Finally, the inter- and intra-reliability using the Vincent method were relatively lower than in a previous cadaveric study (ICC = 0.96) [5]. This lower reliability can be attributed to the difficulty in identifying the meniscal borders with little anatomical separations, especially in MMPRT with large MME. Observers should standardise the meniscus outer border, such as the meniscosynovial rim [16], in addition to adjusting the MRI intensity to low-signal intra-meniscus and high-signal extra-meniscus. Despite these limitations, open 3D MRI-based reconstruction can provide accurate meniscal volume and visualisation of meniscal translation with the MM bulging.

This study is clinically relevant in that 3D MRI can be used to clarify the mechanism of the swelling and posteromedial extrusion of MM in MMPRT knees. This 3D method using SYNAPSE VINCENT® could help surgeons to improve surgical techniques including pullout repairs [10, 11, 19] and to evaluate the surgical outcome via postoperative MMV and MMEV changes.

Conclusions

This comparative analysis demonstrated that the estimated maximum length and posterior height of MM were greater with 3D MRI than with 2D MRI measurements, indicating that 3D MRI can precisely evaluate the meniscal size including its dimension and volume. This study also revealed the enlargement of MMV and MMEV in MMPRT knees, which is attributed to a biomechanical failure of load transmission and degenerative change in the meniscus.

Compliance with ethical standards

Conflict of interest The authors report no conflicts of interest.

Ethical approval All procedures performed in studies involving human participants were in accordance with the ethical standards of the institutional review board.

References

1. Allaire R, Muriuki M, Gilbertson L, Harner CD (2008) Biomechanical consequences of a tear of the posterior root of the medial meniscus. Similar to total meniscectomy. J Bone Joint Surg Am 90:1922–1931
2. Bloecker K, Guermazi A, Wirth W, Benichou O, Kwoh CK, Hunter DJ, Englund M, Resch H, Eckstein F (2013) Tibial coverage, meniscus position, size and damage in knees discordant for joint space narrowing e data from the Osteoarthritis Initiative. Osteoarthr Cartil 21:419e27
3. Bloecker K, Wirth W, Guermazi A, Hitzl W, Hunter DJ, Eckstein F (2015) Longitudinal change in quantitative meniscus measurements in knee osteoarthritis-data from the Osteoarthritis Initiative. Eur Radiol 25:2960–2968
4. Bloecker K, Wirth W, Hudelmaier M, Burgkart R, Frobell R, Eckstein F (2012) Morphometric differences between the medial and lateral meniscus in healthy men—a three-dimensional analysis using magnetic resonance imaging. Cells Tissues Organs 195:353–364
5. Bowers ME, Tung GA, Fleming BC, Crisco JJ, Rey J (2007) Quantification of meniscal volume by segmentation of 3T magnetic resonance images. J Biomech 40:2811–2815
6. Carpenter JE, Wojtys EM, Houston LJ (1993) Preoperative sizing of meniscal allografts. Arthroscopy 9:344
7. Choi SH, Bae S, Ji SK, Chang MJ (2012) The MRI findings of meniscal root tear of the medial meniscus: emphasis on coronal, sagittal and axial images. Knee Surg Sports Traumatol Arthrosc 20:2098–2103
8. Doumouchtsis SK, Nazarian DA, Gauthaman N, Durnea CM, Munneke G (2017) Three-dimensional volume rendering of pelvic models and paraurethral masses based on MRI cross-sectional images. Int Urogynecol J 28:1579–1587
9. Dube B, Bowes MA, Kingsbury SR, Hensor EMA, Muzumdar S, Conaghan PG (2018) Where does meniscal damage progress most rapidly? An analysis using three-dimensional shape models on data from the Osteoarthritis Initiative. Osteoarthr Cartil 26:62–71
10. Fujii M, Furumatsu T, Kodama Y, Miyazawa S, Hino T, Kamatsuki Y, Yamada K, Ozaki T (2017) A novel suture technique using the FasT-fix combined with Ultrabraid for pullout repair of the medial meniscus posterior root tear. Eur J Orthop Surg Traumatol 27:559–562
11. Furumatsu T, Kodama Y, Fujii M, Tanaka T, Hino T, Kamatsuki Y, Yamada K, Miyazawa S, Ozaki T (2017) A new aiming guide can create the tibial tunnel at favorable position in transtibial pullout repair for the medial meniscus posterior root tear. Orthop Traumatol Surg Res 103:367–371
12. Furumatsu T, Fujii M, Kodama Y, Ozaki T (2017) A giraffe neck sign of the medial meniscus: a characteristic finding of the medial meniscus posterior root tear on magnetic resonance imaging. J Orthop Sci 22:731–736
13. Furumatsu T, Miyazawa S, Tanaka T, Okada Y, Fujii M, Ozaki T (2014) Postoperative change in medial meniscal length in concurrent all-inside meniscus repair with anterior cruciate ligament reconstruction. Int Orthop 38:1393–1399
14. Hughes FW (2005) Archimedes revisited: a faster, better, cheaper method of accurately measuring the volume of small objects. Phys Educ 40:468–474

15. Inoue H, Furumatsu T, Miyazawa S, Fujii M, Kodama Y, Ozaki T (2018) Improvement in the medial meniscus posterior shift following anterior cruciate ligament reconstruction. Knee Surg Sports Traumatol Arthrosc 26:434–441

16. Jones LD, Mellon SJ, Kruger N, Monk AP, Price AJ, Beard DJ (2018) Medial meniscal extrusion: a validation study comparing different methods of assessment. Knee Surg Sports Traumatol Arthrosc 26:1152–1157

17. Khan U, Yasin A, Abid M, Shafi I, Khan SA (2018) A methodological review of 3D reconstruction techniques in tomographic imaging. J Med Syst 42:190

18. Kim JG, Lee YS, Bae TS, Ha JK, Lee DH, Kim YJ, Ra HJ (2013) Tibiofemoral contact mechanics following posterior root of medial meniscus tear, repair, meniscectomy, and allograft transplantation. Knee Surg Sports Traumatol Arthrosc 21:2121–2125

19. Kodama Y, Furumatsu T, Fujii M, Tanaka T, Miyazawa S, Ozaki T (2016) Pullout repair of a medial meniscus posterior root tear using a FasT-fix all-inside suture technique. Orthop Traumatol Surg Res 102:951–954

20. Kwak YH, Lee S, Lee MC, Han HS (2018) Large meniscus extrusion ratio is a poor prognostic factor of conservative treatment for medial meniscus posterior root tear. Knee Surg Sports Traumatol Arthrosc 26:781–786

21. LaPrade CM, Ellman MB, Rasmussen MT, James EW, Wijdicks CA, Engebretsen L, LaPrade RF (2014) Anatomy of the anterior root attachments of the medial and lateral menisci: a quantitative analysis. Am J Sports Med 42:2386–2392

22. LaPrade CM, James EW, Cram TR, Feagin JA, Engebretsen L, LaPrade RF (2015) Meniscal root tears: a classification system based on tear morphology. Am J Sports Med 43:363–369

23. McDermott ID, Sharifi F, Bull AM, Gupte CM, Thomas RW, Amis AA (2004) An anatomical study of meniscal allograft sizing. Knee Surg Sports Traumatol Arthrosc 12:130–135

24. Okazaki Y, Furumatsu T, Miyazawa S, Kodama Y, Kamatsuki Y, Hino T, Masuda S, Ozaki T (2019) Meniscal repair concurrent with anterior cruciate ligament reconstruction restores posterior shift of the medial meniscus in the knee-flexed position. Knee Surg Sports Traumatol Arthrosc 27:361–368

25. Otsubo H, Akatsuka Y, Takashima H, Suzuki T, Suzuki D, Kamiya T, Ikeda Y, Matsumura T, Yamashita T, Shino K (2016) MRI depiction and 3D visualization of three anterior cruciate ligament bundles. Clin Anat 30:276–283

26. Ozkoc G, Circi E, Gonc U, Irgit K, Pourbagher A, Tandogan RN (2008) Radial tears in the root of the posterior horn of the medial meniscus. Knee Surg Sports Traumatol Arthrosc 16:849–854

27. Padalecki JR, Jansson KS, Smith SD, Dornan GJ, Pierce CM, Wijdicks CA, Laprade RF (2014) Biomechanical consequences of a complete radial tear adjacent to the medial meniscus posterior root attachment site: in situ pull-out repair restores derangement of joint mechanics. Am J Sports Med 42:699–707

28. Park do Y, Min BH, Choi BH, Kim YJ, Kim M, Suh-Kim H, Kim JH (2015) The degeneration of meniscus roots is accompanied by fibrocartilage formation, which may precede meniscus root tears in osteoarthritic knees. Am J Sports Med 43:3034e44

29. Roth M, Emmanuel K, Wirth W, Kwoh CK, Hunter DJ, Eckstein F (2018) Sensitivity to change and association of three-dimensional meniscal measures with radiographic joint space width loss in rapid clinical progression of knee osteoarthritis. Eur Radiol 28:1844–1853

30. Seitz AM, Lubomierski A, Friemert B, Ignatius A, Durselen L (2012) Effect of partial meniscectomy at the medial posterior horn on tibiofemoral contact mechanics and meniscal hoop strains in human knees. J Orthop Res 30:934–942

31. Shaffer B, Kennedy S, Klimkiewicz J, Yao L (2000) Preoperative sizing of meniscal allografts in meniscus transplantation. Am J Sports Med 28:524–533

32. Shrout PE, Fleiss JL (1979) Intraclass correlations: uses in assessing rater reliability. Psychol Bull 86:420–428

33. Svensson F, Felson DT, Zhang F, Guermazi A, Roemar FW, Niu J, Aliabadi P, Neogi T, Englund M (2019) Meniscal body extrusion and cartilage coverage in middle-aged and elderly without radiographic knee osteoarthritis. Eur Radiol 29:1848–1854

34. Wenger A, Wirth W, Hudelmaier M, Noebauer-Huhmann I, Trattnig S, Bloecker K et al (2013) Meniscus body position, size, and shape in persons with and persons without radiographic knee osteoarthritis: quantitative analyses of knee magnetic resonance images from the osteoarthritis initiative. Arthritis Rheum 65:1804e11

35. Wirth W, Frobell RB, Souza RB, Li X, Wyman BT, Le Graverand MP, Link TM, Majumdar S, Eckstein F (2010) A three-dimensional quantitative method to measure meniscus shape, position, and signal intensity using MR images: a pilot study and preliminary results in knee osteoarthritis. Magn Reson Med 63:1162–1171

36. Yao J, Lancianese SL, Hovinga KR, Lee J, Lerner AL (2008) Magnetic resonance image analysis of meniscal translation and tibio-menisco-femoral contact in deep knee flexion. J Orthop Res 26:673–684

Affiliations

Yoshiki Okazaki[1] · Takayuki Furumatsu[1] · Takuya Yamaguchi[2] · Yuya Kodama[3] · Yusuke Kamatsuki[1] · Shin Masuda[1] · Yuki Okazaki[1] · Takaaki Hiranaka[1] · Ximing Zhang[1] · Toshifumi Ozaki[1]

Yoshiki Okazaki
yokazaki218@gmail.com

Takuya Yamaguchi
yamagu-t@okayama-u.ac.jp

Yuya Kodama
ykodama314@gmail.com

Yusuke Kamatsuki
fufu9youfu@yahoo.co.jp

Shin Masuda
me18066@s.okayama-u.ac.jp

Yuki Okazaki
yokazaki.okayama@gmail.com

Takaaki Hiranaka
koumei.01.13@gmail.com

Ximing Zhang
zhangximing1993@hotmail.com

Toshifumi Ozaki
tozaki@md.okayama-u.ac.jp

1   Department of Orthopaedic Surgery, Okayama
    University Graduate School, 2-5-1 Shikata-cho, Kitaku,
    Okayama 700-8558, Japan

2   Division of Radiology, Medical Technology Department,
    Okayama University Hospital, 2-5-1 Shikata-cho, Kitaku,
    Okayama 700-8558, Japan

3   Department of Orthopaedic Surgery, Iwakuni Medical
    Center, 1-1-1 Atago-machi, Iwakuni, Yamaguchi 740-8510,
    Japan